

# Internal Tin Nb<sub>3</sub>Sn Conductors Engineered for Fusion and Particle Accelerator Applications

Jeff A. Parrell, Youzhu Zhang, Mike B. Field, Maarten Meinesz, Yibing Huang, Hanping Miao, Seung Hong, Najib Cheggour, and Loren Goodrich

**Abstract**—The critical current density ( $J_c$ ) of Nb<sub>3</sub>Sn strand has been significantly improved over the last several years. For most magnet applications, high  $J_c$  internal tin has displaced bronze process strand. The highest  $J_c$  values are obtained from distributed barrier strands. We have continued development of strands made with Nb-47wt%Ti rods to supply the dopant, and have achieved  $J_c$  values of 3000 A/mm<sup>2</sup> (12 T, 4.2 K). Such wires have very good higher field performance as well, reaching 1700 A/mm<sup>2</sup> at 15 T. To reduce the effective filament diameter in these high  $J_c$  strands, the number of subelement rods incorporated into the final restack billet has been increased to 127 in routine production, and results are presented on experimental 217 stacks. A new re-extrusion technique for improving the monofilament shape is also described. For fusion applications such as ITER, we have developed single-barrier internal tin strands having non-Cu  $J_c$  values over 1100 A/mm<sup>2</sup> (12 T, 4.2 K) with hysteresis losses less than 700 mJ/cm<sup>3</sup> over non-Cu volume. The  $J_c$ -strain behavior of such composites is also presented.

**Index Terms**—Internal tin, Nb<sub>3</sub>Sn, superconducting materials.

## I. INTRODUCTION

THE notable performance gains realized for internal tin Nb<sub>3</sub>Sn strands over the past decade are the result of a consistent, sustained development program that has set goals for strand performance that were well beyond the state of the art. Funding from the US Department of Energy for conductors for high field accelerator magnets, coupled with commercial investment for conductors for ever-higher field NMR (nuclear magnetic resonance) magnets, lead to a period of substantial improvement in Nb<sub>3</sub>Sn technology. We are now in a period where magnet designers and builders are learning how to take advantage of the very highest performance wire, in a variety of magnet applications where high  $J_c$  alone may not be sufficient [1], [2]. As part of this transition from innovation to application, our recent activities have focused on engineering high  $J_c$

strands to meet the customized needs of a variety of magnet applications.

At the present time, Oxford Superconducting Technology (OST) manufactures two types of Nb<sub>3</sub>Sn strand using internal tin processes. OST used to manufacture a considerable quantity of strand via the bronze process as well, but for many applications internal tin strand is now favored since its  $J_c$  can be nearly four times that of bronze wire.

The internal tin strands we produce today are most easily described as having either a distributed or single diffusion barrier (the barrier prevents tin from diffusing into the matrix copper). In the case of distributed barrier strand, each subelement of the restack billet contains a tin core and is surrounded by its own diffusion barrier, also made of Nb. Our Restacked Rod Process (RRP) wire is an example of a distributed barrier wire, and the high Nb and Sn fractions that are possible in such a design account for the high non-Cu  $J_c$  values [3]–[5]. This type of strand has been developed for High Energy Physics (HEP) and NMR applications. In the case of single barrier strand, a lone Ta diffusion barrier surrounds all of the tin-bearing subelement rods that comprise the restack billet. Since the attainable Nb and Sn fractions are lower for this wire type than for the distributed barrier wire, the non-Cu  $J_c$  values are correspondingly lower. However, strand made by the single barrier method can have lower hysteresis losses, since the dimensions of its superconducting regions can be made smaller than for the distributed barrier case (i.e. micron-scale Nb<sub>3</sub>Sn filaments vs. Nb<sub>3</sub>Sn tubes or rings that are tens of microns in diameter). We have been developing the single barrier type of strand for use in low hysteresis loss applications such as ITER.

## II. DEVELOPMENT OF DISTRIBUTED BARRIER STRAND (RRP)

### A. Critical Current Density Variation

Since its development in 2002, production volumes of high  $J_c$  RRP strand have grown to tons per year. One of our standard strands is made with Nb-7.5wt%Ta, in a billet configuration (restack hex pattern) of 61 subelement rods. Some copper is usually left at the center of the billet, so typically either 54 or 60 of the 61 hex rods in the stack contain superconductor (the rest being copper). In short hand notation, these restack configurations are referred to as 54/61 or 60/61 stacks.

Fig. 1 shows the distribution of 12 T and 15 T  $J_c$  values for 61 stack high  $J_c$  RRP billets produced from 2002–2008. Note the values are not self field corrected, but as all of the data comes from  $\sim 0.8$  mm strand, relative comparisons can be made. The samples were heat treated with a final stage at  $\sim 665$  °C, in a temperature range that optimizes the 12 T  $J_c$ . (note that it is

Manuscript received August 21, 2008. First published June 05, 2009; current version published July 15, 2009. This work was supported in part by the High Energy Physics Division of DOE through Lawrence Berkeley National Laboratory (Contract DE-AC03-76SF00098).

J. A. Parrell, Y. Zhang, M. B. Field, M. Meinesz, Y. Huang, H. Miao, and S. Hong are with Oxford Instruments, Superconducting Technology, Carteret, NJ 07008 USA (e-mail: jeff.parrell@oxinst.com; youzhu.zhang@oxinst.com; mike.field@oxinst.com; maarten.meinesz@oxinst.com; yibing.huang@oxinst.com; hanping.miao@oxinst.com; seung.hong@oxinst.com).

N. Cheggour and L. Goodrich are with the Oxford Instruments, Superconducting Technology, Carteret, NJ 07008 USA, and also with the National Institute of Standards and Technology, Boulder, CO 80305 USA (e-mail: cheggour@boulder.nist.gov; goodrich@boulder.nist.gov).

Digital Object Identifier 10.1109/TASC.2009.2018074

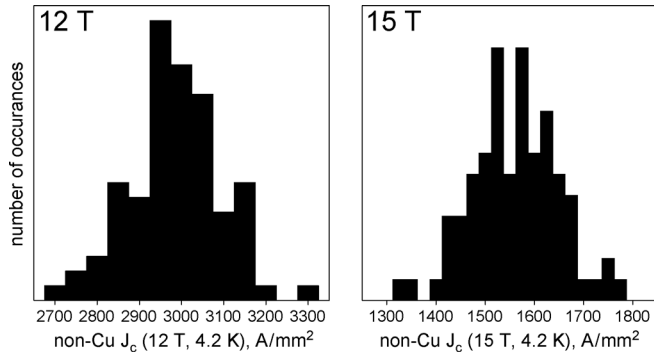


Fig. 1. Non-Cu  $J_c$  (4.2 K) distributions for high  $J_c$  Nb-Ta RRP billets at 12 T (left) and 15 T (right). The samples were heat treated between 650–675 °C, so as to optimize  $J_c$  values in the low field regime ( $\sim$ 12 T).

possible to improve the higher field  $J_c$  values by heat treating the strand at higher temperatures, e.g. 675–700 °C [5], [6]. As the distribution in  $J_c$  values has not changed over time [7], suggesting that the observed  $\sim$ 11% variation (for three standard deviations) for the 12 T  $J_c$  values is a limit of manufacturing reproducibility. This variation likely reflects several factors, including extrinsic variations of  $J_c$  sample preparation and testing, and perhaps practical limits of control of the metal fraction (Nb/Sn/Cu) within the superconducting subelement, as well as intrinsic variations in the Nb alloy itself (and probably the Sn and Cu as well). The 15 T  $J_c$  variation is somewhat larger ( $\sim$ 17%), and perhaps this reflects a greater contribution from variation in the strain state of the wire on the Ti test mandrels.

### B. Reduced Effective Filament Diameter

For some applications, such as accelerator magnets, the strand must carry high currents in regions of low magnetic field. Although the stability of a wire in low fields is not solely dependent on the filament size, the effective filament diameter ( $D_{\text{eff}}$ ) is a factor of primary importance [8], [9]. In recent years, the standard RRP billet for HEP use has been a 54/61 stack configuration, meaning the strand has 54 subelements that each effectively act as a single filament after reaction to Nb<sub>3</sub>Sn. We have been working to increase the number of subelement rods in the final restack billet, for applications that require a smaller  $D_{\text{eff}}$ .

While the restack billet fabrication process is in principle the same regardless of the subelement rod count, there are some manufacturing challenges associated with increasing the rod count much above 100. Internal tin billets cannot be extruded (since tin would melt), so they are processed by cold drawing. This results in a restriction on the billet aspect ratio, since drawing of large diameter, short rods leads to poor yield, and therefore internal tin restack billets typically have an initial length/diameter ratio  $>$ 50. For a given restack billet size (diameter and length), it becomes more and more difficult to increase the subelement rod count, since although the rods need to be smaller in area (hex size), their length needs to stay the same in order to make a commercial scale billet ( $>$ 30 kg). Rods of small cross section, when combined with a

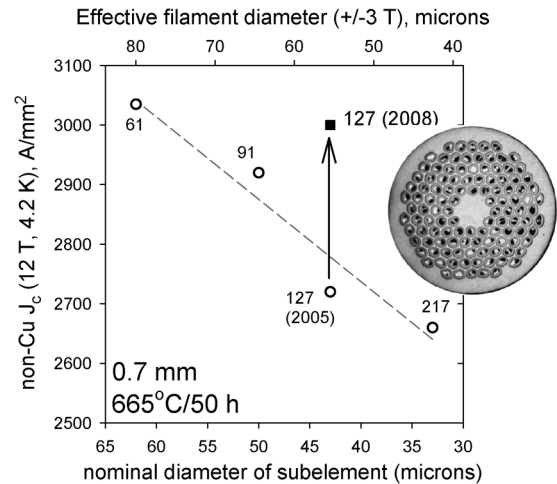


Fig. 2.  $J_c$  data as a function of subelement diameter for (open symbols) wire results from 2005 [5] and today (solid square). A picture of the 114/127 stack strand is also shown (0.7 mm diameter).

length/diameter ratio greater than  $\sim$ 1500, are difficult to handle and keep organized in a billet packing pattern. We are in the process of developing techniques to handle higher subelement count billets.

To meet the needs of the US LHC Accelerator Research Program (LARP), we have worked on and have had good success at increasing the number of rods in the restack billet from 61 to 127 [7]. As our restack billet designs have been refined (management of rod/tube interface areas), billet assembly techniques improved (rod cleaning and handling), and wire cross section made more uniform (drawing schedule modification [10]), we have seen an improvement in the attainable  $J_c$  compared with results we have reported previously. Fig. 2 shows our prior  $J_c$  results for a series of 61, 91, 127, and 217 stack billets [5], along with data typical for the 127 stacks produced today. The improved processing has resulted in approximately 10% higher  $J_c$ .

Despite the improvements in recent 127 stack billets, even a greater number of subelement rods are needed to reach the US HEP goal of  $D_{\text{eff}} <$  40  $\mu\text{m}$  in 0.7 mm wire [11]. For this reason we continue to develop 217 stack billets for the US Conductor Development Program. Although piecelength continues to be challenge to commercial scale up, we can produce R&D quantities of material.

Fig. 3 shows  $J_c$  as a function of magnetic field, as well as a wire cross section prior to reaction, for a recent development 217 stack, along with data for 61 and 127 stacks made from the same subelement material. At a diameter of 0.7 mm, the 217 stack billet had  $D_{\text{eff}}(\pm 3 \text{ T}) = 41 \mu\text{m}$ . The subelement used Nb-47wt%Ti rods to supply the dopant to pure Nb filaments and barrier [12], instead of the Nb-Ta alloy typically used. In a 61 stack configuration, the subelement gave non-Cu  $J_c$  (12 T, 4.2 K) values of  $\sim$  3000 A/mm<sup>2</sup>. Nearly the same  $J_c$  was achieved in a 127 stack of the same subelement, in agreement with the results reported above for Nb-Ta alloy billets. However in a 217 stack configuration,  $J_c$  is reduced by 10% at 12 T, and

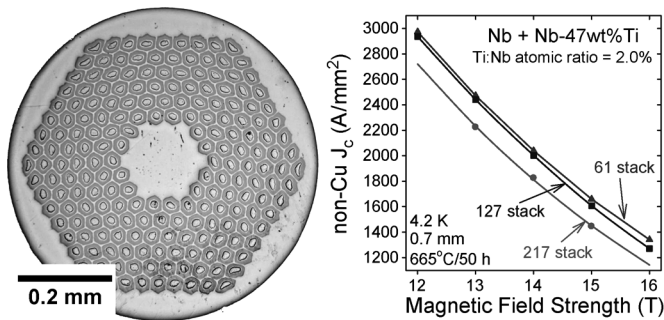


Fig. 3. Cross section of a 217 stack RRP strand, and  $J_c$  data as a function of magnetic field for 61, 127, and 217 stack billets all made from the same Nb + Nb-Ti subelement. While the  $J_c$ -B performance of the 127 stack is close but not quite as good as the 61 stack, the performance decrease for the 217 stack is even more pronounced.

by 15% at 16 T. Over the same 61-127-217 stack series, RRR also decreased, from 124 to 76 to 15.

These results further demonstrate that subelement designs optimized for high  $J_c$  and RRR in 61 stack wire  $\sim 0.7$  mm in diameter, are not optimized for 217 stack billets.  $J_c$  may be limited by poor tin diffusion resulting from pinch-off of the very thin copper layers between monofilament rods upon Nb<sub>3</sub>Sn formation, resulting in tin composition gradients (note the 16 T  $J_c$  values are reduced by a greater percentage than the 12 T values), while RRR may be limited by the thickness of the diffusion barrier. Although modification of the subelement design will be needed to try to achieve high  $J_c$  and RRR in e.g. 0.7 mm strand, the present 217 stack wire performance may be good enough for use at larger wire size e.g. 1 mm, where the subelement size would be closer to the relative size of 61 stack material at 0.7 mm diameter.

### C. Improving Nb Filament Shape by Re-Extrusion Process

The US LARP team has set near term minimum strand performance targets of 12 T  $J_c = 3000$  A/mm<sup>2</sup>, and 15 T  $J_c = 1650$  A/mm<sup>2</sup>, combined with good RRR and low field stability [13]. As can be ascertained from Fig. 1, while a good fraction of the billets produced today would meet these  $J_c$  requirements, the majority would not. Since the variation at 15 T is about 15% (for three standard deviations from the average), the average  $J_c$  would need to be increased by a like amount in order to be able to consistently deliver (i.e. guarantee) those  $J_c$  levels for future applications. Thus, average values of 12 T  $J_c \sim 3300$  A/mm<sup>2</sup> and 15 T  $J_c \sim 1850$  A/mm<sup>2</sup> are needed, to give headroom for manufacturing variation.

As the  $J_c$  depends strongly on the Nb fraction [5], further increases in the Nb fraction are one avenue for exploration, provided that enough Sn can be provided for full conversion to (nearly) stoichiometric Nb<sub>3</sub>Sn [14]. If stoichiometric Nb<sub>3</sub>Sn cannot be formed due to lack of Sn or Sn concentration gradients, then the overall non-Cu  $J_c$  may not improve, even as more Nb and Sn are added to the composite. It is an unanswered question as to whether further  $J_c$  improvements can be made in RRP strands via copper fraction reduction within the subelements, or if the result would be a condition similar to the case for powder-in-tube and internal tin rod-in-tube process strands,

where significant Sn gradients across thick Nb layers limits the maximum possible  $J_c$  [15], [16].

If we are to remove more copper from within the RRP subelement, reduction of the copper between each Nb monofilament is required. As there is little strain space for grain refinement between the melt diameter and the starting monofilament billet diameter, the grain size in Nb bars is typically large, with a large size distribution. Due to the body centered cubic crystal structure of Nb, and the resulting manner in which the grains irregularly deform [17], a large grain size leads to filaments of irregular shape. During drawing to final size, localized areas of thin copper separation become thinner still, to the point where adjacent Nb filaments can come into contact. Such a localized change along a length of wire results in wire breakage. We have observed better piecelength from billets having a rounder monofilament shape compared with billets having more irregular filament shapes. To be able to make the copper thinner still around each Nb rod, while still having a process that is suitable for large scale manufacturing, the filament shape needs to be better controlled.

To try to improve the roundness of the filaments, we have experimented with the processing of the Nb bar, including melt method modification (e.g. electron beam melted vs. electrode arc melted), and changing the route from casting to finished bar (e.g. forging vs. extrusion). However, these efforts have not been very successful, due to the limited strain space between melt ingot size and our starting Nb bar size in monofilament billets. Although reducing the bar diameter would allow for increased strain space for grain-refining thermomechanical processing, it is desirable from an economic point of view to keep the starting monofilament billet size as large as possible.

We are presently experimenting with an alternate route to develop round filament shapes from commercial-scale monofilament billets, following from an observation made earlier by Gregory and Pyon [18]. The “re-extrusion” concept is summarized as follows: 1) extrude a Cu-clad Nb billet from large diameter to an intermediate size, letting the Nb filament shape take on its “natural” shape, depending on the grain structure; 2) machine the copper off the resulting rod, and then machine the Nb bar surface again to a round shape; 3) use this extruded and machined Nb bar as feedstock into our normal monofilament billet processing (re-extrusion). Although extrusion of Nb bar has been tried before as a method of improving the filament shape, key to this new process is the use of the Cu jacket for the initial Nb ingot breakdown. If the Nb is extruded directly, the extrusion die forces the Nb bar into a round shape, but this round shape is not maintained when the Nb is subsequently processed in a Cu jacket. In contrast, the soft Cu allows the Nb grains to freely change shape, and then the irregular filament “fingers” are machined away. After the Nb bar has been allowed to deform as dictated by the grain structure, and the bar has been made round again by machining, the round filament shape can now be maintained in subsequent processing.

As a first experiment, we used 25 mm diameter Cu-clad Nb rod as the starting material, as shown in Fig. 4, for the “as extruded” case. This material had a very irregular filament shape, much worse than typically observed, but therefore a good candidate for this trial. The copper was then machined from a piece

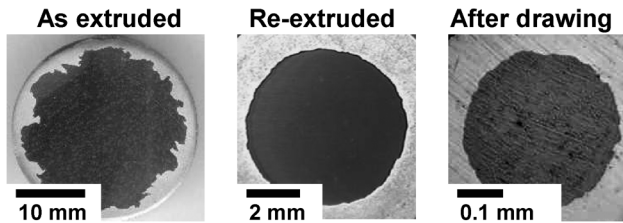


Fig. 4. Nb filaments shapes after initial extrusion (left), after machining to round Nb bar and re-extruding (center), and after drawing (right). Machining Nb after its first extrusion in a copper jacket is an effective means to improve the filament shape.

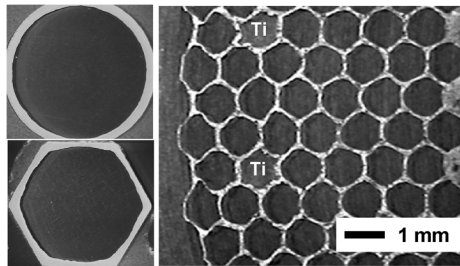


Fig. 5. Cross sections of re-extruded round monofilament (top left), the same material formed to hex shape (bottom left), and RRP subelement made from the hex rod (right). Nb-47Ti rod locations are indicated by “Ti”. The Nb rod shape and copper separation thickness are both uniform in the subelement.

of the rod, and further machined until a smooth, round Nb surface was formed. This machined Nb bar was then put into a new Cu extrusion jacket, and again extruded (the “re-extruded” case in Fig. 5.). The round, smooth filament shape was retained after re-extrusion. The rod was then drawn to small diameter to see if the round filament shape would be maintained after significant strain. As shown in Fig. 4. (the “after drawing” instance), the round shape was maintained.

In a follow on scale up experiment, we started with Cu-clad Nb rod that had been processed to 58 mm diameter. Sections of this material were machined to create round Nb rods suitable for re-extrusion in Cu jackets. Several pieces were re-extruded, drawn to hexagonal shape, and restacked to create a short, but full diameter size, RRP subelement billet. Nb-47Ti rods were used in the billet to provide a Ti dopant source. Cross sections of the re-extruded round monofilament, the final hex rod, and the resulting extruded subelement, are shown in Fig. 5. Note the uniform thickness of the Cu that separates each Nb filament within the subelement.

While much work remains to scale this Nb monofilament re-extrusion process to meet the needs of commercial production, the method may enable experiments to determine the limits of copper removal (from the non-Cu area of the subelement) as a means of  $J_c$  improvement in RRP strand.

### III. PROGRESS WITH SINGLE BARRIER STRAND (ITER)

As the strand development phase of the ITER project has approached completion, we have focused on making small optimizations to a few proven billet designs. All billet types are made with filaments of pure Nb. While we continue to see

good results from billets where the Ti dopant is supplied by Nb-wt%47Ti rods [19], we have also continued to work with more conventional Sn-Ti designs. Our objective is meeting the specifications for both toroidal field (TF) and central solenoid (CS) strand.

Over the past few years, we have supplied several domestic agencies with small ( $\sim 100$  kg) quantities of strand made to their own specification. Typical requirements have included non-Cu  $J_c$  levels  $> 1000$  A/mm<sup>2</sup> (12 T, 4.2 K), and non-Cu hysteresis losses  $< 1000$  mJ/cm<sup>3</sup> ( $\pm 3$  T) [20], and in one case even higher  $J_c$  ( $> 1100$  A/mm<sup>2</sup>) was required [21]. Recently, uniform strand requirements were issued by the ITER International Organization, with the  $J_c$  requirement substantially reduced, to  $\sim 700$  A/mm<sup>2</sup>. These values were reflected in the new TF strand technical specification from Fusion For Energy, the European Union ITER domestic agency [22]. The ITER specification also requires a successful full size CICC (cable in conduit conductor) sample test as a condition of strand acceptance. Unfortunately, as there are additional manufacturing steps between finished strand and a cable test (e.g. cabling and jacketing), and since the cable sample preparation and testing are complicated processes [23], [24], the relationship between single strand performance and the CICC results is not straightforward to discern. As a result, it is not certain that meeting or exceeding the individual TF strand performance parameters will actually result in a strand that is accepted for use in the ITER TF CICC.

It seems a natural consequence of the brittle nature of Nb<sub>3</sub>Sn that higher  $J_c$  wires, having a higher fraction of Nb<sub>3</sub>Sn with less copper separation, should be more susceptible to strain damage than lower performance strands [25]–[27]. This needs to be considered whenever Nb<sub>3</sub>Sn strands are used [1], [2], and indeed very good performance in a CICC can be achieved when strand is well supported [28], [29]. However, since the ITER TF CICC dimensional envelope and operating conditions are fixed, and therefore cable configuration options may be limited, we have been working to create strand more resistant to bending damage. We have been working on two approaches to achieve this: the first is to make the strand more tolerant of a bending strain, and second is to make the strand more resistant to bending stress (i.e. reinforce the strand so that it strains less for a given stress).

#### A. Strain Tolerance of Lower $J_c$ Strand

Since Nb<sub>3</sub>Sn itself is a brittle compound, ceramic engineering techniques may provide a route to improving the bending strain tolerance. As there is some evidence that copper retained between filaments after conversion to Nb<sub>3</sub>Sn performs a crack blunting function [30], we are experimenting with placing more copper between the Nb filaments. We fabricated two subelement billets having the same number of filaments, located at the same positions, but varied the Nb rod diameter to give different copper spacing between filaments. The average spacing between the filaments rings was thereby increased by 17%, and the spacing between filaments within a ring increased by 6%. This resulted in the two subelement billets having different Nb fractions, with the Nb area fraction of the “Low Nb” subelement billet being 6% lower than the “High Nb” billet. The tin fraction of the Low

TABLE I  
HIGH Nb AND LOW Nb BILLET DATA

	Higher Nb fractions	Lower Nb fraction
Heat treatment ending with*	650°C/100h	650°C/200h
Non-Cu J <sub>c</sub> (12 T, 4.2 K)	1100 ± 37 A/mm <sup>2</sup>	951 ± 71 A/mm <sup>2</sup>
Non-Cu hysteresis losses (± 3 T)	679 ± 35 mJ/cm <sup>3</sup>	514 ± 110 mJ/cm <sup>3</sup>
Intrinsic irreversible strain limit (0.1 μV/cm)	0.16-0.19% (two tests)	0.13-0.17% (two tests)

\* Full schedule: 210 °C/50 h + 340 °C/25 h + 450 °C/25 h + 575 °C/100 h + 650 °C/xxx

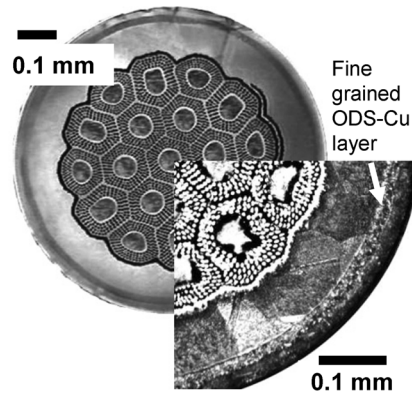


Fig. 6. ODS-Cu reinforced ITER strand, before and after heat treatment. The strengthened copper is in the form of a tube positioned near the strand edge.

Nb billet was also reduced, roughly in proportion to the Nb content.

Subelement rods of both High and Low Nb content were restacked and finished to 0.82 mm strand using our standard 19-stack billet configuration, without tin or copper spacers [5]. The High Nb strand was heat treated using the standard 100 h ITER schedule [22], since its peak J<sub>c</sub> was obtained in a shorter time, while the Low Nb strand was heat treated using the optional 200 h ITER schedule in order to minimize the residual Nb cores within the Nb<sub>3</sub>Sn filaments. For all samples, the ITER specified ramp rate of 5 °C/hour was used. Several samples of each billet type were tested for J<sub>c</sub> and hysteresis losses. Two I<sub>c</sub>-strain samples of each type were tested on a “spring probe” at NIST [31]. The results are summarized in Table I.

Although the average J<sub>c</sub> and losses were reduced between the High and Low Nb billets, the intrinsic irreversible strain limit was not improved, or may have slightly decreased. The observed variation in J<sub>c</sub> and losses was also greater for the Low Nb billet, for reasons not completely understood at this time. SEM analysis of the microstructures of these wires revealed that the filaments in the Low Nb strand were fully reacted, but the results may indicate the Nb<sub>3</sub>Sn is less homogeneous due to the reduced Sn content of the billet [13]. In any case, the fact that the tensile strain irreversibility limit was not improved may indicate that still thicker copper is needed between filaments for improved strain tolerance, and therefore that the J<sub>c</sub> of the strand needs to be further reduced to see much effect. We are now producing strands that have even lower J<sub>c</sub> to test this hypothesis.

*B. Development of Reinforced Strand*

As an alternative to trying to improve the strain tolerance, we have also produced strand intended to have greater resistance to bending stresses. A thin annulus of oxide dispersion strengthened (ODS) copper was incorporated with the copper pipe used as the restack jacket for our ITER billets. This tube of reinforcing material, positioned near the perimeter of the strand, is intended to strengthen the strand against bending stress. A thin layer of copper was provided at the outer edge of the strand, so that wire drawing and Cr plating would still occur against a pure Cu surface, rather than the ODS-Cu. The ODS-Cu fraction was 20% of the copper matrix area, or 10% of the overall strand cross section since the billets have a Cu:non-Cu ratio ~1.0. Fig. 6

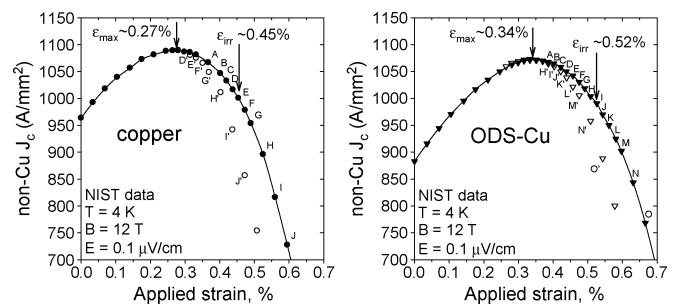


Fig. 7. Non-Cu J<sub>c</sub> data as a function of applied strain, for plain copper-sheathed and ODS-Cu reinforced ITER strands. The ODS-Cu strand has a higher irreversible strain point.

shows cross sections of this strand, before and after heat treatment.

A billet was produced using this ODS-Cu reinforced copper restack tube, and the High Nb subelement described earlier. The billet was drawn as usual, with very good piecelength, and showed no sign of drawing problems or mechanical difficulties. Samples of the strand were heat treated with the short 650 °C/100 h schedule, and tested as described above. J<sub>c</sub>-strain measurements for both the ODS-Cu strand, and the High Nb strand described earlier, are shown Fig. 7. As the two strands were made from a common subelement, nominally the only difference between the two strands was the ODS-Cu layer present in the copper matrix. Note that the NIST apparatus does not provide for stress-free cooling of the sample since the latter is soldered to a Cu-Be spring. Despite the additional compressive pre-strain applied on the sample by the spring during cooling (from the soldering temperature to 4 K), the comparison in Fig. 7 does serve to illustrate the fact that the ODS-Cu causes three changes relative to the strand having a pure Cu matrix: first, that the J<sub>c</sub> at zero applied strain is reduced; second, the position of the J<sub>c</sub> peak on the strain curve shifted to a higher value of applied strain (as a result of the additional precompression supplied by the ODS-Cu [32]), and third, the irreversible strain limit is increased, even though the intrinsic irreversible strain limit remained unchanged.

Although the effect of the ODS-Cu was clear in the J<sub>c</sub>-strain characteristic (a measure of the longitudinal strain behavior), it remains to be seen if the strand would be more bend resistant

or tolerant in the CICC. Tensile measurements at 77 K showed little difference between the plain copper and the ODS-Cu jacketed strands, up to a tensile strain of 0.8%. This is consistent with the fact that the elastic modulus of the ODS-Cu is similar to that of pure Cu, and that the strengthened copper comprised only about 10% of the strand cross section. Although additional tests of the strand would be needed to see if the strengthened sheath helps under actual CICC operating conditions, this method of reinforcing strand appear to be straightforward to implement, and could be accomplished at a modest cost.

#### IV. SUMMARY

We have continued development of distributed barrier conductors for HEP applications. The  $J_c$  performance of RRP strands has been consistent over time, indicating a stable design and robust manufacturing process. A reduction of the effective filament diameter is still needed for HEP use, and we now can maintain the highest  $J_c$  values in restack billets containing 127 subelements. Restacks containing still finer subelements are in development, with  $J_c$  values in 217 subelement count restack billets typically  $\sim 10\%$  lower than the best values. An improvement in the Nb monofilament shape may lead to further progress with  $J_c$ , piecelength, and effective filament diameter reduction in RRP strands. We are investigating the commercial feasibility of a new monofilament re-extrusion process to achieve Nb filament shapes that are more rounded, with initial positive results.

We are also developing single barrier conductors intended for use in ITER. The relationship between the  $J_c$  and hysteresis losses, and the strain sensitivity of these strands is not straightforward. Refinements in the subelement design may lead to improvements in strain tolerance. The use of strengthened copper alloy may also be a cost effective method of improving the strain tolerance of strands for use in CICCs.

#### ACKNOWLEDGMENT

The authors would like to thank the groups at the National High Magnetic Field Laboratory, and the Applied Superconductivity Center at NHMFL, for 77 K tensile measurements and detailed microstructural investigations. NHMFL is supported by NSF Cooperative Agreement No. DMR-0084173, by the State of Florida, and by the DOE. They would also like to thank their many colleagues at the Lawrence Berkeley, Brookhaven, and Fermi National Accelerator Laboratories for technical discussions and their consistent support of strand development for HEP use, as well as US ITER (at Oak Ridge National Laboratory) and Fusion For Energy for their support of ITER strand development.

#### REFERENCES

[1] A. Twin, J. Brown, F. Domptail, R. Bateman, R. Harrison, M. Lakrimi, Z. Melhem, P. Noonan, M. Field, S. Hong, K. Marken, H. Miao, J. Parrell, and Y. Zhang, "Present and future applications for advanced superconducting materials in high field magnets," *IEEE Trans. Appl. Supercond.*, vol. 17, no. 2, pp. 2295–2298, 2007.

[2] A. Vostner, P. Bauer, R. Wesche, U. Besi Vetrella, B. Stepanov, A. della Corte, A. Portone, E. Salpietro, and P. Bruzzone, "Qualification of the EFDA dipole high field conductor," *IEEE Trans. Appl. Supercond.*, vol. 18, no. 2, pp. 544–547, 2008.

[3] J. A. Parrell, Y. Zhang, M. B. Field, and S. Hong, "High field Nb<sub>3</sub>Sn conductor development at Oxford Superconducting Technology," *IEEE Trans. Appl. Supercond.*, vol. 13, pp. 3470–3473, 2002.

[4] M. Field, J. Parrell, Y. Zhang, and S. Hong, "Critical Current Density in Nb<sub>3</sub>Sn Superconducting Wire," U.S. Patent 7368021, May 6, 2008.

[5] J. A. Parrell, Y. Zhang, M. B. Field, and S. Hong, "Development of internal tin Nb<sub>3</sub>Sn conductor for fusion and particle accelerator applications," *IEEE Trans. Appl. Supercond.*, vol. 17, no. 2, pp. 2560–2563, 2007.

[6] A. K. Ghosh, L. D. Cooley, J. A. Parrell, M. B. Field, Y. Zhang, and S. Hong, "Effects of reaction temperature and alloying on performance of restack-rod-process Nb<sub>3</sub>Sn," *IEEE Trans. Appl. Supercond.*, vol. 17, no. 2, pp. 2623–2626, 2007.

[7] M. B. Field, J. A. Parrell, Y. Zhang, M. Meinesz, and S. Hong, "Internal tin Nb<sub>3</sub>Sn conductors for particle accelerator and fusion applications," *Adv. Cryo. Engr.*, vol. 54, pp. 237–243, 2008.

[8] V. V. Kashikhin and A. V. Zlobin, "Magnetic instabilities in Nb<sub>3</sub>Sn strands and cables," *IEEE Trans. Appl. Supercond.*, vol. 15, no. 2, pp. 1621–1624, 2005.

[9] A. V. Zlobin, V. V. Kashikhin, and E. Barzi, "Effect of flux jumps in superconductor on Nb<sub>3</sub>Sn accelerator magnet performance," *IEEE Trans. Appl. Supercond.*, vol. 16, no. 2, pp. 1308–1311, 2006.

[10] M. B. Field, J. A. Parrell, Y. Zhang, and S. Hong, "Nb<sub>3</sub>Sn conductor development for fusion and particle accelerator applications," *Adv. Cryo. Engr.*, vol. 52, pp. 544–549, 2006.

[11] R. M. Scanlan, D. R. Dietderich, and S. A. Gourley, "A new generation Nb<sub>3</sub>Sn wire, and the prospects for its use in particle accelerators," *Adv. Cryo. Engr.*, vol. 50B, pp. 349–358, 2004.

[12] S. Hong, J. Parrell, and M. Field, "Method for Producing (Nb,Ti)3Sn Wire by Use of Ti Source Rods," U.S. Patent 6981309, January 3, 2006.

[13] US LHC Accelerator Research Program, Specification No. LARP-MAG-M-8002, Rev. A, Mar. 2008.

[14] P. J. Lee and D. C. Larbalestier, "Microstructural factors important for the development of high critical current density Nb<sub>3</sub>Sn strand," *Cryogenics*, vol. 48, pp. 283–292, 2008.

[15] C. D. Hawes, P. J. Lee, and D. C. Larbalestier, "Measurements of the microstructural, microchemical, and transition temperature gradients of A15 layers in a high-performance Nb<sub>3</sub>Sn powder-in-tube superconducting strand," *Supercond. Sci. Technol.*, vol. 19, pp. S27–S37, 2006.

[16] X. Peng, M. D. Sumption, R. Dhaka, M. Bhatia, M. Tomsic, E. Gregory, and E. W. Collings, "Composition profiles and upper critical field measurement of internal Sn and tube type conductors," *IEEE Trans. Appl. Supercond.*, vol. 17, no. 2, pp. 2668–2671, 2007.

[17] R. Heussner, P. Lee, and D. Larbalestier, "Nonuniform deformation of niobium diffusion barriers in niobium-titanium wire," *IEEE Trans. Appl. Supercond.*, vol. 3, pp. 757–760, 1993.

[18] E. Gregory and T. Pyon, unpublished.

[19] J. A. Parrell, M. B. Field, Y. Zhang, and S. Hong, "Advances in Nb<sub>3</sub>Sn strand for fusion and particle accelerator applications," *IEEE Trans. Appl. Supercond.*, vol. 15, no. 2, pp. 1200–1204, 2005.

[20] A. Vostner and E. Salpietro, "Enhanced critical current densities in Nb<sub>3</sub>Sn superconductors for large magnets," *Supercond. Sci. Technol.*, vol. 19, pp. S90–S95, 2006.

[21] A. Vostner and E. Salpietro, "The European Nb<sub>3</sub>Sn advanced strand development programme," *Fusion Eng. Des.*, vol. 75–79, p. 169, 2005.

[22] Fusion For Energy, Call for Tender No. F4E-2008-OPE-05 (MS-MG), Supply of Chromium Plated Nb<sub>3</sub>Sn Strand, Jul. 2008.

[23] P. Bruzzone, M. Bagnasco, D. Ciazynski, A. della Corte, A. Di Zenobio, R. Herzog, Y. Ilyin, B. Lacroix, L. Muzzi, A. Nijhuis, B. Renard, E. Salpietro, L. S. Richard, B. Stepanov, S. Turtù, A. Vostner, R. Wesche, L. Zani, and R. Zanino, "Test results of two ITER TF conductor short samples using high current density Nb<sub>3</sub>Sn strands," *IEEE Trans. Appl. Supercond.*, vol. 17, no. 2, pp. 1370–1373, 2007.

[24] L. Savoldi Richard and R. Zanino, "Application of calorimetry to the assessment of the performance of ITER Nb<sub>3</sub>Sn TF conductor samples in SULTAN tests," *Supercond. Sci. Technol.*, vol. 21, p. 105004, 2008.

[25] X. Feng Lu, S. Pragnell, and D. Hampshire, "Small reversible axial-strain window for the critical current of a high performance Nb<sub>3</sub>Sn superconducting strand," *Appl. Phys. Lett.*, vol. 91, p. 132512, 2007.

[26] A. Nijhuis, Y. Ilyin, W. Abbas, W. A. J. Wessel, and H. J. G. Krooshoop, "Performance of ITER (EU-TFPRO-2) Nb<sub>3</sub>Sn strands under spatial periodic bending, axial strain and contact stress," *IEEE Trans. Appl. Supercond.*, vol. 18, no. 2, pp. 1059–1062, 2008.

- [27] N. Cheggour, L. F. Goodrich, T. C. Stauffer, B. J. Filla, and J. D. Splett, "Irreversible strain limit of ITER  $\text{Nb}_3\text{Sn}$  strands," presented at the LTSW, South Lake Tahoe, CA, Oct. 2007, unpublished.
- [28] P. Bruzzone, M. Bagnasco, M. Calvi, F. Cau, D. Ciazynski, A. della Corte, A. Di Zenobio, L. Muzzi, A. Nijhuis, E. Salpietro, L. Savoldi Richard, S. Turtù, A. Vostner, R. Wesche, and R. Zanino, "Test results of two European ITER TF conductor samples in SULTAN," *IEEE Trans. Appl. Supercond.*, vol. 18, no. 2, pp. 1088–1091, 2008.
- [29] A. Nijhuis, "A solution for transverse load degradation in ITER  $\text{Nb}_3\text{Sn}$  CICC: Verification of cabling effect on Lorentz force response," *Supercond. Sci. Technol.*, vol. 21, p. 054011, 2008.
- [30] M. Jewell, P. J. Lee, and D. C. Larbalestier, unpublished.
- [31] N. Cheggour, L. F. Goodrich, T. C. Stauffer, B. J. Filla, and J. D. Splett, "A probe for measuring critical-current in superconductors as a function of strain, temperature, and magnetic field," presented at the MEM07 Workshop, Princeton, NJ, Aug. 2007, unpublished.
- [32] J. W. Ekin, N. Cheggour, M. Abrecht, C. Clickner, M. Field, S. Hong, J. Parrell, and Y. Zhang, "Compressive pre-strain in high niobium fraction  $\text{Nb}_3\text{Sn}$  superconductors," *IEEE Trans. Appl. Supercond.*, vol. 15, no. 2, pp. 3560–3563, 2005.